An improvement of the transient voltage assessment method of the DC receiving-end considering access of high-proportion photovoltaic

Zhiyu Chen*, Jianbo Yi, Jia Wang, Shuyi Wang, Changxuan Liu
School of Mechanical & Electrical Engineering, University of Electronic Science and Technology of China, Chengdu 611731, Sichuan, China

ABSTRACT

High-proportion photovoltaic feeding into the DC (Direct Current) receiving end grid makes it very easy to cause DC phase change failure, or even DC blocking and other faults after disturbances occur at the receiving terminal, and its transient voltage stability problem is very prominent, so it is of great significance to quantitatively evaluate the transient voltage stability of DC receiving terminal system. Firstly, we analyze the complex transient characteristics of the DC receiving end after large-scale new energy feed-in, then based on the existing multi-binary table criterion and the transient characteristics of the DC system, and taking into account the transient voltage changes brought by the new energy feed-in, we proposed a three-stage transient voltage assessment method with transient fast recovery, transient slow recovery and transient overvoltage using the idea of assigning different weights to the different transient phases to achieve the assessment of the transient voltage stability. Finally, the applicability of the three-stage transient voltage assessment method to DC system is verified based on the PV receiving end grid with different penetration rates and the receiving end system after the improvement of PV reactive power compensation capacity, and the results show that the proposed method can realize the effective assessment of transient voltage stability of DC receiving end system with large-scale new energy.

Keywords: Transient voltage stability, renewable energy, multi-binary table, transient characteristics

1. INTRODUCTION

In recent years, photovoltaic power generation technology has undergone unprecedented development and is now connected to the power system on a large scale. In China, a new type of power system is being formed: new energy sources such as photovoltaics are connected to the DC receiving end of the grid on a large scale through power electronic equipment, resulting in changes in the transient voltage stability characteristics of the system.

While recognizing the mechanism of transient voltage stability, domestic and foreign scholars have proposed a number of quantitative evaluation methods for transient voltage in order to determine the voltage stability quickly and effectively. Reference[1] uses the critical fault removal time as the transient voltage stability index; Reference[2] uses the energy function to solve the unstable equilibrium point of the system. In addition, many scholars have devoted themselves to the study of the practical criterion of transient voltage stabilization in index form. Reference[3] mentions the use of multi-binary table criterion to construct transient voltage dip acceptability index based on transient voltage offset threshold and maximum acceptable duration. In this paper, a three-stage transient voltage assessment quantification method for large-scale PV-fed DC receiving system is proposed based on the multi-binary table criterion and the transient recovery characteristics of the DC system, and the transient voltage stability of the DC system is verified under different PV penetration rates and PV reactive power optimization compensation.

2. TRANSIENT VOLTAGE CHARACTERISTICS OF LARGE-SCALE PHOTOVOLTAIC FEEDTHROUGHS TO DC RECEIVERS

With the access of large-scale new energy sources, the transient voltage stability of the HVDC (High Voltage Direct Current) receiving end is affected, especially its transient characteristics during faults are changed. According to the quasi-steady state model of DC system, the relationship of each electrical quantity in the inverter side is as follows:

*202221040322@std.uestc.edu.cn

Fifth International Conference on Green Energy, Environment, and Sustainable Development (GEESD 2024), edited by M. Aghaei, X. Zhang, H. Ren, Proc. of SPIE Vol. 13279, 132790F · © 2024 SPIE · 0277-786X
 · doi: 10.1117/12.3044588

$$P_{\mathrm{d}} = U_d I_d = N\left(\frac{3\sqrt{2}}{\pi} K V_C \cos\gamma - \frac{3}{\pi} I_d X_C\right) I_d \tag{1}$$

$$Q_d = P_{\mathrm{d}} \tan\varphi = P_{\mathrm{d}} \tan\left[\arccos\left(\cos\gamma - \frac{I_d X_C}{\sqrt{2} K V_C}\right)\right] \tag{2}$$

$$I_d = (U_{dr} - U_{di}) / X_d \tag{3}$$

$$Q_a = Q_d - Q_c = Q_d - B V_C^2 \tag{4}$$

where: P_{d} is the DC delivered power; Q_{d} is the reactive power consumed by the converter on the inverter side; Q_{a} is the total reactive power exchange of the AC and DC system; Q_{c} is the reactive power issued by the compensation equipment in the converter station; U_{d}, I_{d} are the DC voltage and current; U_{dr}, U_{di} are the rectifier-side and inverter-side DC voltages, respectively; V_{C} is the converter bus voltage; φ is the converter transformer ratio; γ is the inverter converter off angle; X_{C}, X_{d} are the equivalent phase change reactance of the inverter side and the equivalent impedance of the DC transmission line, respectively; B is the equivalent power of reactive power compensation equipment[4].

It can be seen that the stability of the DC receiver voltage is strongly related to the dynamic characteristics of its reactive power. In the event of a fault in the receiving end system, it may lead to phase change failure on the DC side. In the study of transient characteristics of DC receiving end voltage, the transient process is often studied by dividing it into the fault period and the fault recovery period. The DC reactive-voltage characteristics of these two phases are analyzed below.

2.1 Analysis of reactive power-voltage characteristics during faults

The fault will cause the inverter side commutation bus voltage to drop, which will cause the inverter side DC voltage to drop rapidly as shown in D-E. From equation (3), it can be seen that (U_{dr}-U_{di}) becomes larger, and the DC current increases sharply in a short time, resulting in a short-term overcurrent, and $I_{\mathrm{d}}>I_{\mathrm{d0}}$. At this time, the reactive power required by the DC system increases accordingly, but the reactive power provided by the reactive compensation equipment decreases at a square rate as the commutation bus voltage decreases, that is, $|\Delta Q_{\mathrm{c}}|>|\Delta Q_{\mathrm{d}}|$, then $Q_{\mathrm{a}}>0$ at this time, the DC system absorbs reactive power from the AC system, and the DC at this stage exhibits the characteristics of a reactive load. However, the protection action can act quickly after the fault occurs, and the duration of this stage is short, so the impact on the system is relatively small.

2.2 Reactive power-voltage characterization during fault recovery

After the fault is cleared, the recovery process of the transient voltage is shown in Figure 1a, stages 2 and 3, where the DC inverter side current is gradually recovered under DC control, and the rising stage of its voltage can be divided into the fast recovery F-G section and the slow recovery H-I section in terms of the recovery rate. In the time partition of the two transient phases, the voltage recovery to 0.65 p.u. time is chosen as the split node of the two transient processes in this paper[5-8].

In the fast recovery F-G-H stage, VDCOL has not controlled the adjustment of the current command in time, the DC current at this stage is still in a state of decline, and $I_{\mathrm{d}}<I_{\mathrm{d0}}$. When the DC control is in the dominant role, the current command I_{dref} gradually rises under the action of VDCOL, and the DC current also rises in the process, but the situation of $I_{\mathrm{d}}<I_{\mathrm{d0}}$ still exists. Correspondingly, the rise of the converter bus voltage means that the reactive power compensation capability of the reactive power compensation equipment is rapidly improved and restored, but the lag in the recovery of DC current means that the reactive power consumed by DC is also delayed in the recovery, but at this time, $Q_{\mathrm{a}}<0$. At this stage, the AC system has to bear the excess reactive power of the reactive power compensation equipment, and this process of the DC system exhibits the characteristics of reactive power supply.

When the DC control delay ends, the DC voltage comes to the slow recovery H-I stage: As the converter bus voltage is not restored to the stabilized level at this time, $Q_{\mathrm{c}}<Q_{\mathrm{c0}}$, as the inverter side DC voltage is still lower than the steady-state level, DC current is still small $I_{\mathrm{d}}<I_{\mathrm{d0}}$, the inverter side power factor angle still relatively large, and then we can see that the DC consumed reactive power is higher than the steady state reactive power. Then the AC system output reactive

power Q_a=Q_d-Q_c>0, in this process, the DC system as a reactive load needs to absorb reactive power from the AC system for a long period of time causing the greatest disturbance to the stability of the power system.

When there is a large amount of new energy access in the recipient grid, this paper takes PV as an example, the most characteristic difference in the system response lies in the overvoltage part of the voltage recovery in the H-I-J phase, i.e., the slow recovery phase[9-11]. This can be seen in Figure 1b, which shows that when large-scale PV exists, the DC voltage can rise to 0.65 p.u. in one step fast, but there is an overshooting serious transient overvoltage situation during the recovery process after fault removal. This is due to the reduction of the inverter-side turn-off angle, which causes the voltage to increase, thus increasing the reactive power compensation margin. Therefore, in the case of large-scale new energy connection, the influence of overvoltage should be taken into account. Because the voltage oscillation deviation after overvoltage is small, and the time to converge to the reference voltage is long, its impact on voltage stability is small and negligible. Therefore, this paper simplifies this stage and merges it to the steady state voltage without calculating its influence on the transient voltage stability.

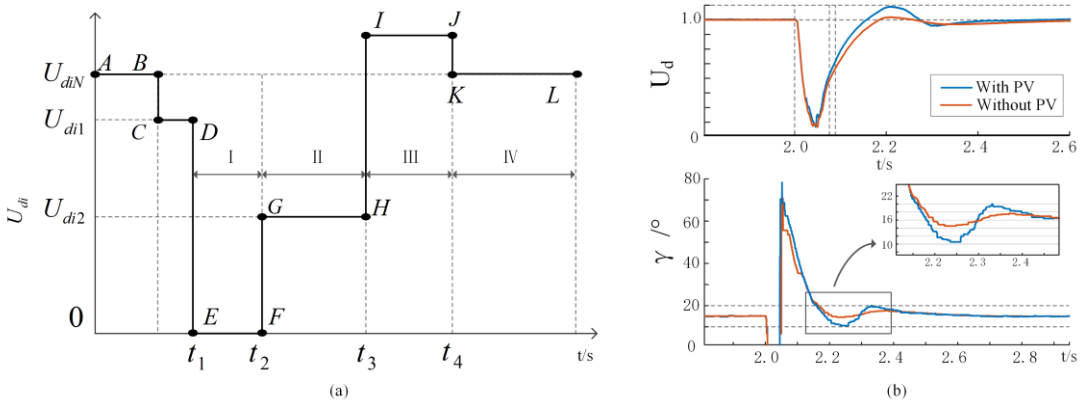

Figure 1. (a): Schematic diagram of DC voltage changes due to commutation failure of inverter; (b): Comparison of influence of large-scale new energy sources on DC voltage recovery.

3. CONSTRUCTION OF EVALUATION INDICATORS BASED ON BINARY TABLES

For the fine quantitative assessment of transient voltage stability margin, the single binary table is too single for the division of voltage dip intervals, so some scholars use multiple binaries to construct the evaluation index. Reference[3] quantifies the transient voltage stability margin defined by assigning different weights to different degrees of voltage drop intervals. However, the paper did not consider the transient overvoltage situation that occurs when a large number of new energy sources are connected to the grid, and lacked the evaluation of new energy sources connected to the grid.

According to the above situation, the transient voltage stability of large-scale photovoltaic access is quantitatively analyzed and evaluated based on the multi-binary table. The transient voltage recovery after fault removal is divided into three stages by these four-time nodes: fast recovery stage, slow recovery stage, and transient overvoltage stage, as shown in Figure 2.

The fast recovery phase is a delayed recovery phase specific to DC transmission systems and is the main reason for the failure of multi-binary meters used by previous scholars due to the low voltage magnitude during this time period. The slow recovery phase is related to the strength of the AC system at the receiving end, the reactive power reserve and also the voltage support capability. When the reactive power margin at the receiving end is sufficient, the voltage can realize faster recovery, therefore, the data index of this phase can well characterize the stability level of transient voltage. The transient overvoltage stage is mainly reflected in the transient overvoltage characteristics of the voltage response, which may cause new energy chain, disorderly high-voltage off-grid accident. With the increase of the proportion of new energy in the receiving end grid, the amplitude of transient overvoltage is larger, which is more unfavorable to the stability of the system.

Based on the multi-binary table method and the transient voltage recovery characteristics of DC systems containing large-scale photovoltaics, this paper proposes a three-stage transient voltage evaluation method applicable to DC systems. The evaluation indexes of the method are composed of three parts, corresponding to the three stages of voltage recovery.

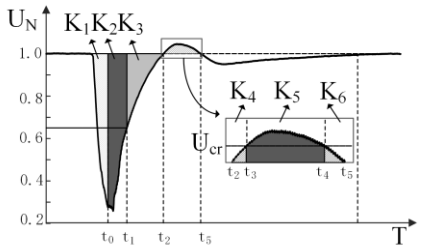

Figure 2. Weighted quantitative analysis based on multi-binary table criterion.

3.1 Localized transient low voltage severity indicator

For the two low-voltage stages after fault removal, they are evaluated quantitatively using the binary table criteria (U_{cr}^{0}, T_{cr}^{0}) and (U_{cr}^{1}, T_{cr}^{1}), the index of the degree of voltage drop after fault removal is:

$$\eta_L = \frac{\int_{t_0}^{t_1}[(U_N - U(t)]\mathrm{d}t}{(U_N - U_{cr}^{0})T_{cr}^{0}} + \frac{\int_{t_1}^{t_2}[(U_N - U(t)]\mathrm{d}t}{(U_N - U_{cr}^{1})T_{cr}^{1}} \tag{5}$$

The binary table judgment consisting of the transient low voltage and the maximum acceptable duration of the transient voltage dip in the above can be adjusted according to the standards related to the practical judgment of the transient voltage dip. In this paper, (0.65 p.u., 0.1 s), (0.9 p.u., 10 s) are used as the base judgment.

3.2 First transient overvoltage severity index

The localized voltage rise severity index for transient voltage response after large-scale PV connection to the receiving grid needs to be described in a fine step:

$$\eta_H = \frac{\int_{t_3}^{t_4}[(U(t) - U_N]\mathrm{d}t}{(U_{cr}^{3} - U_N)T_{cr}^{3}} + \frac{\int_{t_2}^{t_3}[(U(t) - U_N]\mathrm{d}t}{(U_{cr}^{2} - U_N)(t_3 - t_2)} + \frac{\int_{t_4}^{t_5}[(U(t) - U_N]\mathrm{d}t}{(U_{cr}^{2} - U_N)(t_5 - t_4)} \tag{6}$$

3.3 Global transient voltage severity indicator

Based on the whole process of DC transient voltage response, a three-stage transient voltage evaluation method can be constructed as in Equation (7), and it is stipulated that the index exceeds 0.5 system is in a critical instability situation:

$$\begin{aligned}\eta &= \eta_L + \eta_H \\ &= \frac{\int_{t_0}^{t_1}[(U_N - U(t)]\mathrm{d}t}{(U_N - U_{cr}^{0})T_{cr}^{0}} + \frac{\int_{t_1}^{t_2}[(U_N - U(t)]\mathrm{d}t}{(U_N - U_{cr}^{1})T_{cr}^{1}} + \frac{\int_{t_3}^{t_4}[(U(t) - U_N]\mathrm{d}t}{(U_{cr}^{3} - U_N)T_{cr}^{3}} + \frac{\int_{t_2}^{t_3}[(U(t) - U_N]\mathrm{d}t}{(U_{cr}^{2} - U_N)(t_3 - t_2)} + \frac{\int_{t_4}^{t_5}[(U(t) - U_N]\mathrm{d}t}{(U_{cr}^{2} - U_N)(t_5 - t_4)}\end{aligned} \tag{7}$$

4. EXAMPLES AND ANALYSIS

In order to verify the effectiveness and universality of the transient voltage assessment method of the multi-binary meter, the assessment effects of the multi-binary meter and the three-stage transient voltage method proposed in this paper are compared under different PV penetration rates and in PV reactive power compensation optimization systems, respectively. The test system is set up as a simplification of a new HVDC transmission and receiving end system, and the schematic is shown in Figure 3a.

4.1 Transient voltage stability evaluation at different PV penetration rates

In order to verify the differentiation ability of this paper's method under different PV permeability, based on the CIGRE standard DC test model, using the system structure shown in Figure 3a of this paper, the PV permeability is set to 5%-35% for seven groups, respectively, to compare the transient voltage assessment effect of the two methods and the original area integration method under the three-phase short-circuit faults occurring in the system. Figure 3b shows the simulation results of DC transient voltage under different penetration rates[10].

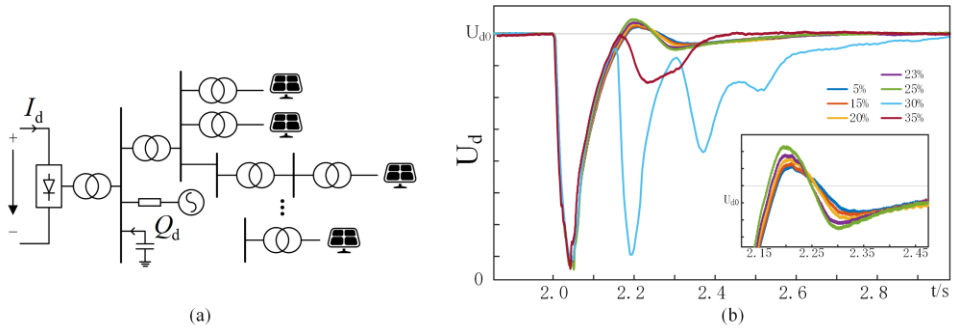

Figure 3. (a): Schematic diagram of new HVDC receiver system; (b): Transient voltage response for different PV penetration rates.

It can be seen from Figure 3 that when the PV penetration rate is lower than 25%, the voltage can be restored to the standard voltage more quickly after fault removal, but its transient overvoltage amplitude increases with the increase of penetration rate, and there is a risk of further deterioration of the transient voltage. As the penetration rate reaches 30%, there is a "secondary transient drop/rise" in the voltage recovery process, which may trigger a chain of off-grid accidents and increase the risk of system-wide fault development. The resultant values of the transient voltage stability assessment using multiple binary tables and trinomials are shown in Table 1.

Table 1. Comparison of multi-binary table and three-stage evaluation of transient voltage stability.

Permeability	Multiple binary table	Three-stage	Primitive integration	State
5%	0.45864	0.28029	0.52054	Stable
15%	0.45807	0.39317	0.58018	Stable
20%	0.45316	0.28473	0.58619	Stable
23%	0.44910	0.28689	0.52504	Stable
25%	0.45103	0.29839	0.58883	Stable
30%	0.45506	0.64322	1.20374	Unstable
35%	3.08692	0.98173	1.84744	Unstable

4.2 Transient voltage stability assessment under PV with reactive power compensation

According to Reference[12] on PV inverters, a reactive voltage control strategy for PV power plants based on active adaptive adjustment is proposed so that the PV power plant has three modes of MPPT, active reduction and static synchronous compensation. In the reactive power compensation optimized PV the same penetration rate, the transient voltage stability case values are displayed in Table 2.

Table 2. Comparison of multi-binary table and three-stage evaluation of transient voltage stability under PV reactive power optimization.

Permeability	Multiple binary table	Three-stage	Primitive integration	State
5%	0.46063	0.30989	0.61373	Stable
15%	0.42234	0.37178	0.64913	Stable
20%	0.41648	0.38104	0.54984	Stable
23%	0.41024	0.28657	0.54028	Stable
25%	0.39595	0.24661	0.53670	Stable

From the comparison of the results in Tables 1 and 2, it can be seen that the stability of the system at 25% penetration is better than 23% after adding the adaptive reactive power adjustment capability. The voltage immunity is enhanced due to the optimized adjustment of its reactive power so that it can output excess reactive power to the HVDC system to help in the fast recovery of the DC voltage when the voltage is reduced. The effectiveness of the literature PV inverter control optimization is verified along with the universality of the evaluation methodology in this paper.

5. CONCLUSION

Large-scale new energy access to the DC receiving end grid will cause transient voltage characteristics to change, this paper constructs a local and global transient voltage assessment method based on multi-binary table for such transient voltage characteristics. Simulation verification is carried out in different PV penetration rate and PV reactive power optimization system, and the results show that the three-stage transient voltage assessment method reduces the misjudgment phenomenon of the traditional multi-binary table transient voltage evaluation method in HVDC system, and is suitable for the rapid quantitative evaluation of transient voltage. However, the applicability to other complex HVDC terminated systems needs to be further analyzed.

REFERENCES

[1] Priyamvada, I. R. S. and Das, S., "Online assessment of transient stability of grid connected PV generator with DC link voltage and reactive power control," IEEE Access 8, 220606-220619 (2020).

[2] Hassan, M., Hossain M. J. and Shah, R., "Impact of meshed HVDC grid operation and control on the dynamics of AC/DC systems," IEEE Systems Journal 15, 5209-5220 (2021).

[3] Zhao, J., Zhu, Y. and Tang, J., "Transient voltage and transient frequency stability emergency coordinated control strategy for the multi-infeed HVDC power grid," 2020 IEEE Power & Energy Society General Meeting (PESGM), Montreal, QC, Canada, 1-5 (2020).

[4] Kim, S. and Overbye, T. J., "Mixed transient stability analysis using AC and DC models," IEEE Transactions on Power Systems 31, 942-948 (2016).

[5] Cheng, T., Lin N. and Dinavahi, V., "Hybrid parallel-in-time-and-space transient stability simulation of large-scale AC/DC grids," IEEE Transactions on Power Systems 37, 4709-4719 (2022).

[6] Priyamvada, I. R. S. and Das, S., "Transient stability of VDC-Q control-based PV generator with voltage support connected to grid modelled as synchronous machine," IEEE Access 8, 130354-130366 (2020).

[7] Tang, G., Xu, Z. and Zhou, Y., "Impacts of three MMC-HVDC configurations on AC system stability under DC line faults," IEEE Transactions on Power Systems 29, 3030-3040 (2014).

[8] Xia, Y., Wei, W., Long, T., Blaabjerg, F. and Wang, P., "New analysis framework for transient stability evaluation of DC microgrids," IEEE Transactions on Smart Grid 11, 2794-2804 (2020).

[9] Lu, H., Liu, Y., Yuan, Y., Deng, W., Su, P. and Jiang, X., "A transient voltage support strategy based on medium voltage photovoltaic grid-connected converter during commutation failure in the LCC-HVDC system," 2023 8th International Conference on Power and Renewable Energy (ICPRE), Shanghai, China, 1658-1664 (2023).

[10] Eftekharnejad, S., Vittal, V., Heydt, G. T., Keel, B. and Loehr, J., "Impact of increased penetration of photovoltaic generation on power systems," IEEE Transactions on Power Systems 28, 893-901 (2013).

[11] You S., et al., "Impact of high PV penetration on the inter-area oscillations in the U.S. eastern interconnection," IEEE Access 5, 4361-4369, (2017).

[12] Zevallos, O. C., Silva, J. B. D., Mancilla-David, F., Neves, F. A. S., Neto, R. C. and Prada, R. B., "Control of photovoltaic inverters for transient and voltage stability enhancement," IEEE Access 9, 44363-44373, (2021).